Supporting Information

Mechanism and Kinetics of Enzymatic Degradation of Polyester Microparticles Using a Shrinking Particle-Shrinking Core Model

Hooman Torabi,[a] Farhad Javi,[a] Ted W Deisenroth,[b] Toan V. Pho,[b] Victoria Barbright,[b] Alireza Abbaspourrad[a]*

[a] Department of Food Science, College of Agriculture & Life Sciences, Cornell University, Stocking Hall, Ithaca, New York, 14853, United States

[b] BASF Corporation, 500 White Plains Road, Tarrytown, New York 10591, United States

* Corresponding Author. Email address: Alireza@cornell.edu (A. Abbaspourrad)

Materials and Methods:

EXPERIMENTAL

Materials

Polybutylene adipate-co-terephthalate (PBAT), Polybutylene Sebacate-co-terephthalate (PBSeT), and Polybutylene succinate (PBS) were provided by BASF (Tarrytown, NY, USA). Novozyme 51032 cutinase enzyme from *Humicola insolens* (15000 Lipase Units g^{-1} (15 kLU g^{-1})) was purchased from Strem Chemicals Inc. (Newburyport, MA, USA). Polycaprolactone (PCL, M_w ~80000 g/mol), Polyvinyl alcohol (PVA, Mowiol 10-98, M_w ~61000 g/mol), Fluorescein sodium, and Tween 80 were all purchased from Sigma-Aldrich (St. Louis, MO, USA). Sodium phosphate monobasic and sodium phosphate dibasic were purchased from Acros chemicals (Pittsburgh, PA, USA) to prepare 50 mM phosphate buffer at pH 7.6. This buffer was used to dilute enzyme stock solution. In all the steps, solvents used were reagent grade. In all the experiments, ultrapure MQ water was used.

Methods

The general method for using our microfluidic device to obtain experimental data regarding enzymatic degradation begins by priming the microfluidic channel with dilute Tween 80 in water (0.25 w/v%) to avoid particles aggregation and consequent clogging the microfluidic channel. Microparticles were dispersed in NaCl solution (~30 w/v%, matched to microparticle density), and containing 0.25 w/v% Tween 80. This mixture was then injected into the microfluidic channel. This process continued until a proper number of particles (10-20) were efficiently trapped and immobilized in the analytical region of the channel. Then, water was flushed through the channel to remove the salt and emulsifier. Finally, the enzyme solution (150 LU g^{-1}- 15 kLU g^{-1}) was introduced to the channel using a syringe pump at constant flow rate of 10 µL h^{-1} the approximate

duration of experiments ranged from 2 to 200 h. For fluorescent imaging, the enzyme solution was spiked with fluorescein sodium salt (2 µg mL^{-1} final concentration). Particles were monitored and the change in their size and appearance was assessed during degradation to provide time-resolved particle conversion information via image processing methods.

Summary of SPM-SCM model

Table S1: Summary of SPM-SCM model with associated RDSs.

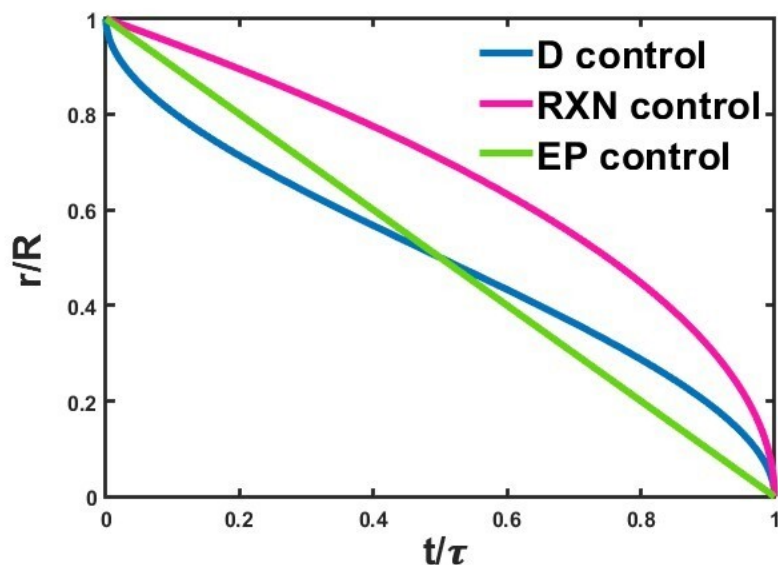| RDS	SPM	SCM
Intermediate formation (EP control)	$t_{EP} = \tau_{EP}\left[1 - \left(\dfrac{r}{R}\right)\right]$ $\tau_{EP} = \dfrac{\varepsilon\rho R}{k_f[E]}$	$t_{EP} = \tau_{EP}\left[1 - \left(\dfrac{r}{R}\right)\right]$ $\tau_{EP} = \dfrac{\varepsilon\rho R}{k_f[E]}$
Bond cleavage (RXN control)	$t_{RXN} = \tau_{RXN}\left[1 - \left(\dfrac{r}{R}\right)^2\right]$ $\tau_{RXN} = \dfrac{A_0}{k^{'}[E]^n}$	$t_{RXN} = \tau_{RXN}\left[1 - \left(\dfrac{r}{R}\right)^2\right]$ $\tau_{RXN} = \dfrac{A_0}{k^{'}[E]^n}$
Diffusion through the ash layer	N/A	$t_D = \tau_D\left[1 - 3\left(\dfrac{r}{R}\right)^2 + 2\left(\dfrac{r}{R}\right)^3\right]$ $\tau_D = \dfrac{\varepsilon\rho R^2}{6D[E]}$

Figure S1: Conversion-time curves with possible RDSs

Microparticle preparation:

The microparticles were prepared via conventional oil-in-water solvent extraction/evaporation method.[1] 100 mL of 4 w/w% PVA was used as the aqueous (continuous) phase. 50 mL of 10 w/v% polymer in chloroform (organic layer) was added dropwise to the aqueous layer held at 45 °C while stirring by mechanical stirrer (IKA Eurostar 40 digital, Germany) at 500 rpm and 700 rpm for particles with radius >20 μm and >10 μm, respectively. After 5 h, particles were filtered by a nylon mesh filter with 15 μm mesh size (U-CMN-15, Component Supply Co., Tennessee, USA) or 38 μm mesh size (U-CMN-38) depending on the desired size range. Finally, particles were washed several times with water and dried via lyophilization. For SEM, samples were coated with gold/palladium using a sputter coater (Denton Desk V, NJ, USA). The coated samples were examined with an SEM (Zeiss Gemini 500, Jena, Germany). Objects were scanned with electron beam (1 keV) and visualized using a high-efficiency secondary-electron detector with a 30.0 μm aperture.
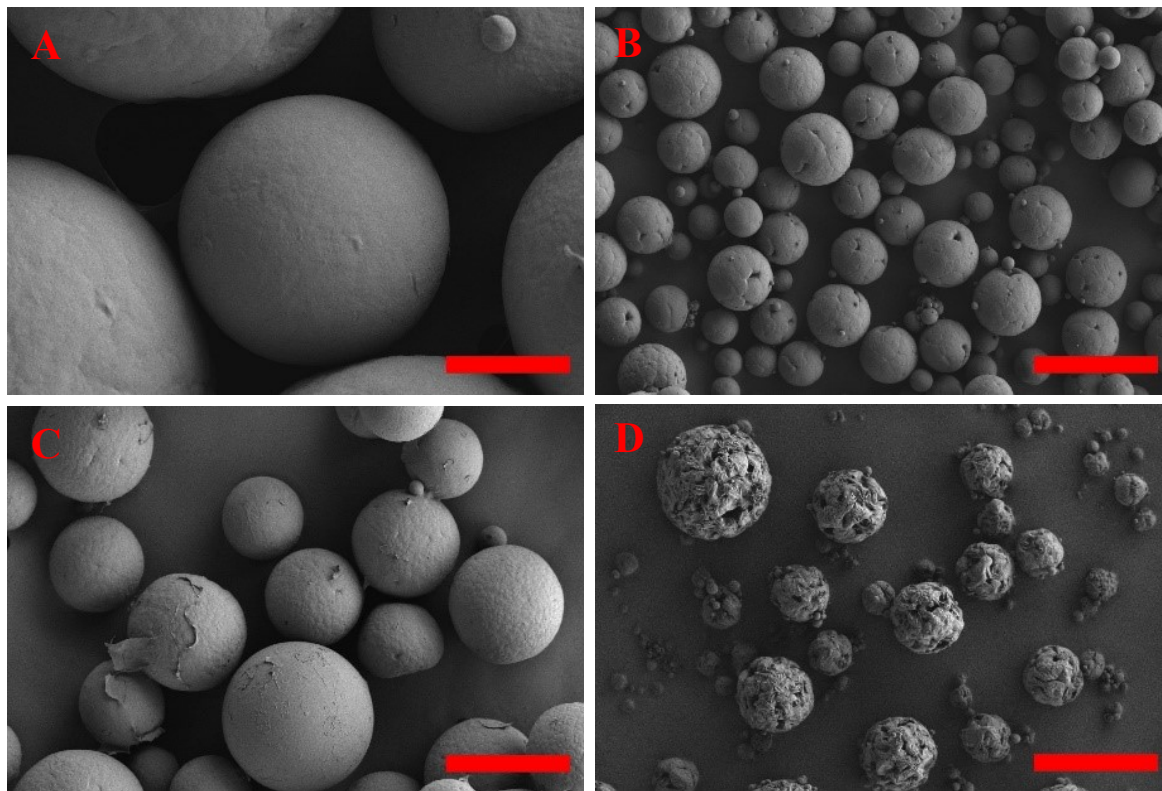
Figure S2: SEM images of A) PCL, B) PBAT, C) PBSeT, D) PBS microparticles. Scale bar is 50 µm

Thermal Properties:

Differential Scanning Calorimetry experiments were performed using Q2000 TA Instruments (New Castle, DE, USA). Samples were heated from room temperature to 200 °C at 10 °C min^{-1} under nitrogen atmosphere. To measure the degree of crystallinity (X_c%) of PBSeT, Wide Angle X-ray Diffraction (WAXD) of its particles were analyzed using a Bruker D8 advanced eco with Cu k alpha X-ray source. Peaks found at 16.2°, 17.5°, 20.5°, 23.3°, and 24.5° correspond to crystal planes of PBSeT (**Figure S3**) and similar to previously reported results.[2]

Table S2: Thermal properties and molecular weight of microparticles

Material	PBAT	PBSeT	PBS	PCL
Degree of Crystallinity* (particle)	9.1	26	41.7	30.6
Degree of Crystallinity*	11.9	-	42.8	35.3
ΔH$_{ref}$ (J g^{-1})**	114 [3]	-	200 [4]	139.5 [5]

*Degree of crystallinity is calculated by dividing the **ΔH$_{fus}$** from DSC analysis by the **ΔH$_{ref}$** (reference values)

****ΔH$_{ref}$ is** the reference **enthalpy of fusion assuming 100% crystallinity of the substrate.**
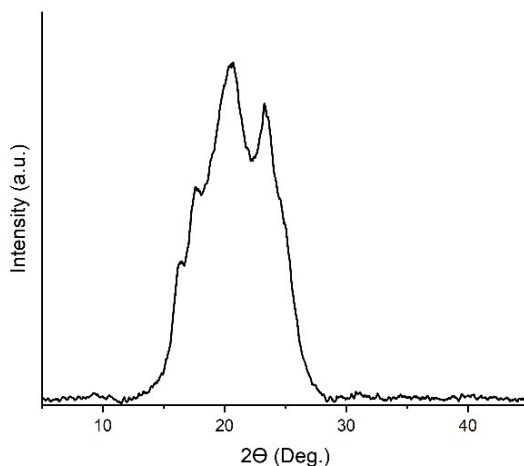

Figure S3: WAXD diffractogram of PBSeT particles

Microfluidic chip design and fabrication:

The channel contains two major regions. A separation region provides a well-dispersed flow of particles. Particles are trapped in the analytical region providing a uniform and statistically representative sample of physically immobilized particles. Enzymatic degradation of the particles was studied monitoring the particles in analytical region. All channels were fabricated via standard lithography methods. [6] [7] In summary, photoresist SU-8 2025 or SU-8 2050 (Microchem) was coated on a silicon wafer for channels with thickness of 35 μm and 50 μm, respectively. The master mold was prepared via UV-photolithography at 350 nm and removal of excess photoresist from wafers. Polydimethylsiloxane (PDMS) chip was prepared by mixing liquid PDMS and curing agent (Sylgard 184) at a 10:1 ratio. This mixture was then casted on the molds and cured for 3 hours. Cured PDMS chips were peeled off, punched, and bonded to glass slides via oxygen plasma bonding technique.
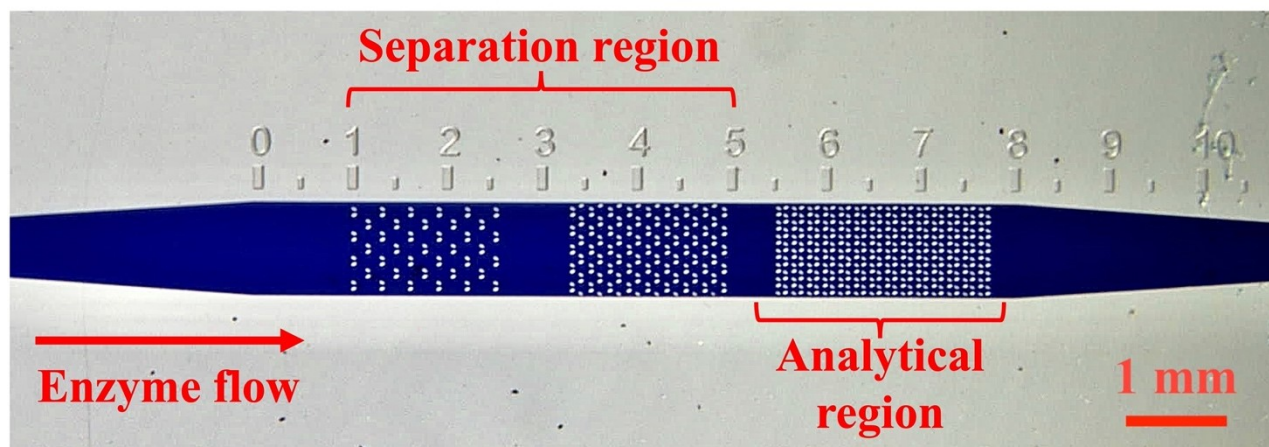

Figure S4: Wide view of the microfluidic channel

Image processing and modeling

Particle and unreacted-core size and darkness were measured over time using ImageJ software (NIH, Bethesda, MD. 1.53q). Mathematical modeling and curve fitting was performed by non-linear least-square regression method (Trust-region algorithm) using Matlab software (Mathworks, Inc. 2022a). OriginPro 2022.b. (OriginLab Corp., Northampton, MA.) was used to perform statistical analysis and prepare some of the figures.
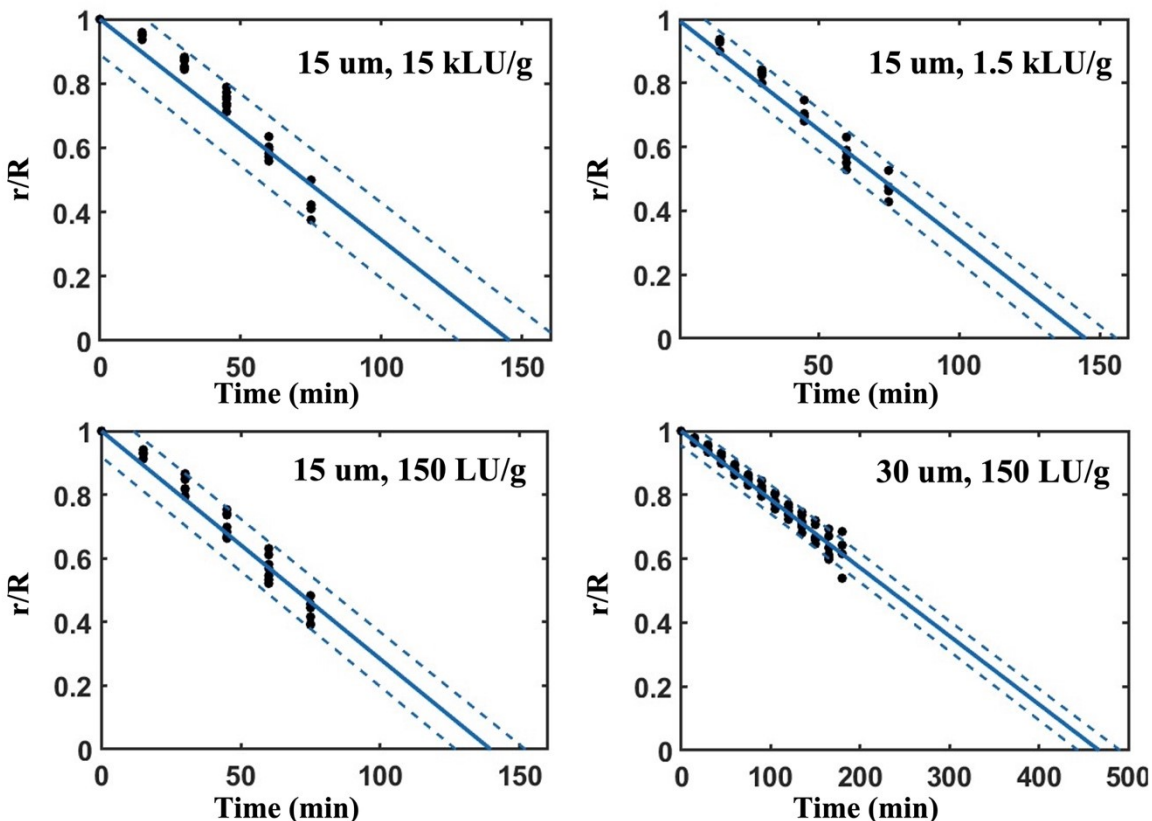
Shrinking particle:

Figure S5: Conversion-time data of enzymatic degradation of PCL micro particles (black dots) and fitted curves with EP control mechanism (blue line). Dashed lines indicate 95% prediction bonds.
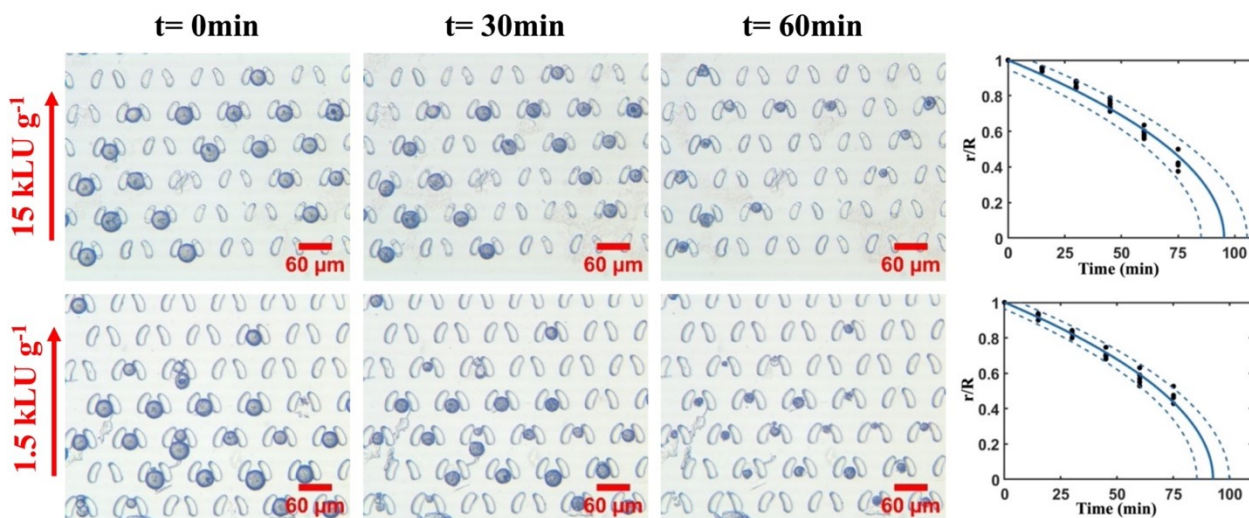

Figure S6: Time lapse of enzymatic degradation of PCL microparticles with ~15 μm in radius using enzyme at 15 LU g^{-1} (top), and 1.5 kLU g^{-1} (bottom). Scale bar is 60 μm.

Table S3: Detailed results of fitting the conversion-time of enzymatic degradation of PCL micro particles with RDS models

RDS	τ (min)							
	15 kLU g^{-1} (15.95 μm)	Fit (R^2)	1.5 kLU g^{-1} (15.6 μm)	Fit (R^2)	150 LU g^{-1} (16.2 μm)	Fit (R^2)	150 LU g^{-1} (28.8 μm)	Fit (R^2)
RXN control :	95.3 ± 1.7	0.9401	92.5 ± 1.3	0.9821	90.9 ± 1.1	0.9792	275.2 ± 2.6	0.9751
EP control :	145.6 ± 4.3	0.8698	145.0 ± 2.9	0.9604	139.6 ± 2.6	0.9623	467.1 ± 5.4	0.9641
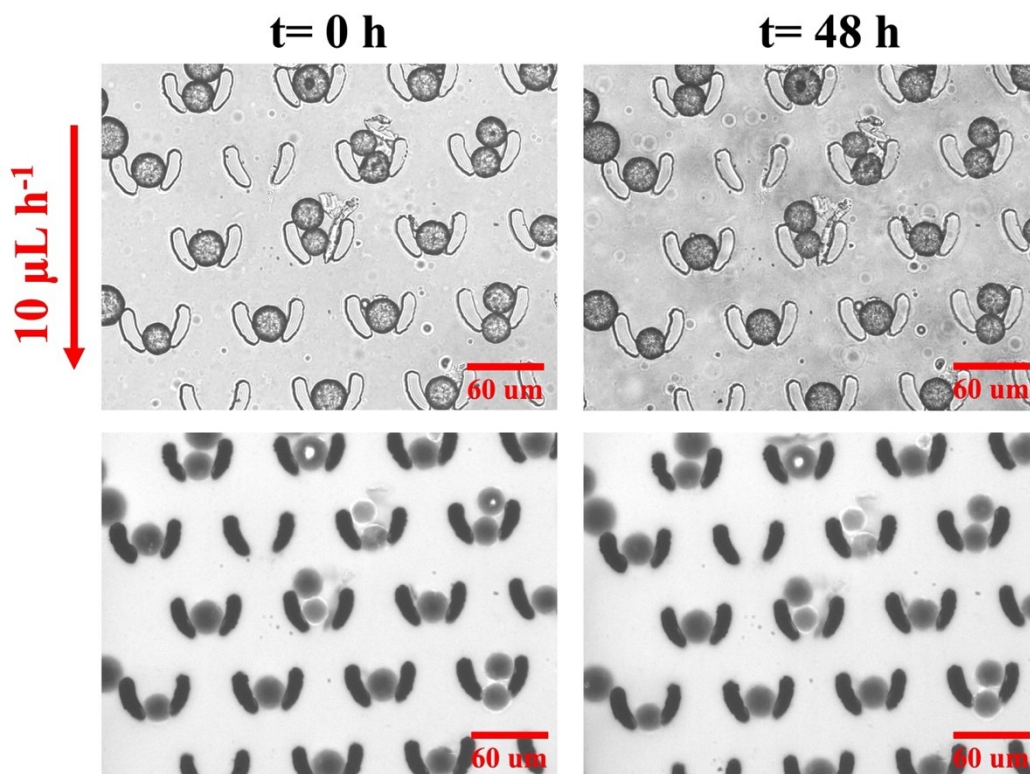
Figure S7: Visible light (top) and fluorescent (bottom) images of PBAT particles (~15 µm) treated with buffer spiked with fluorescent dye.
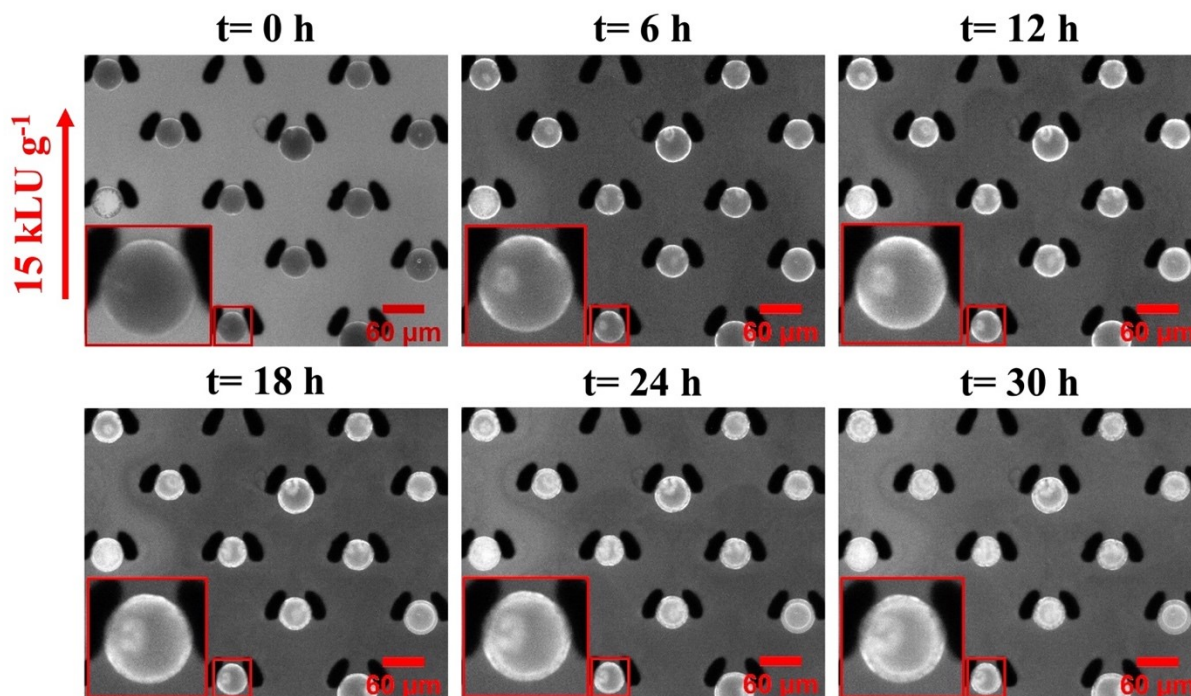

Figure S8: Fluorescent images of PBAT particles (~20 µm) during enzymatic degradation
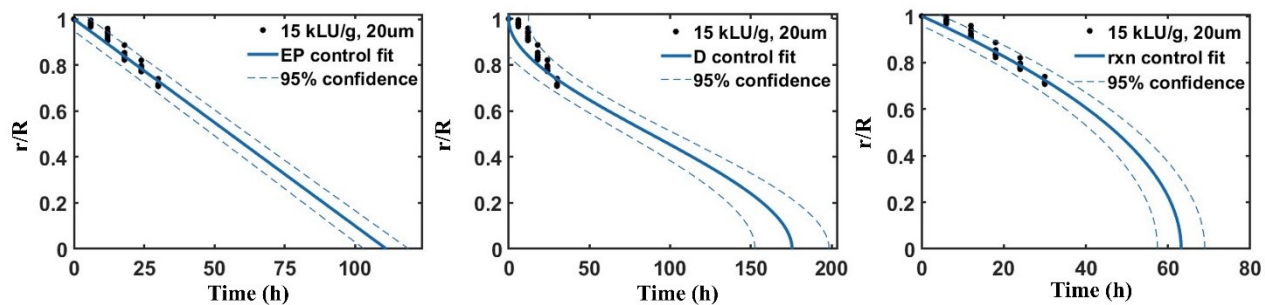
Shrinking core:

Figure S9: Conversion-time data of enzymatic degradation of PBAT micro particles (black dots) and fitted curves with different mechanisms (blue line). Dashed lines indicate 95% prediction bonds.

Table S4: Detailed results of modeling the conversion-time of enzymatic degradation of 20 μm PBAT micro particles at 15kLU g^{-1}

	RDS				
	RXN control:	EP control:	D control:	RXN + D control	EP + D control
τ (h)	63.2 ± 1.37	111.2 ± 2.75	175.4 ± 9.65	$63.2 \pm 1.37 + 4.077\text{e-}09$	$111.2 \pm 2.75 + 4.708\text{e-}14$
Fit (R^2)	0.9417	0.9246	0.6569	0.9417	0.9246

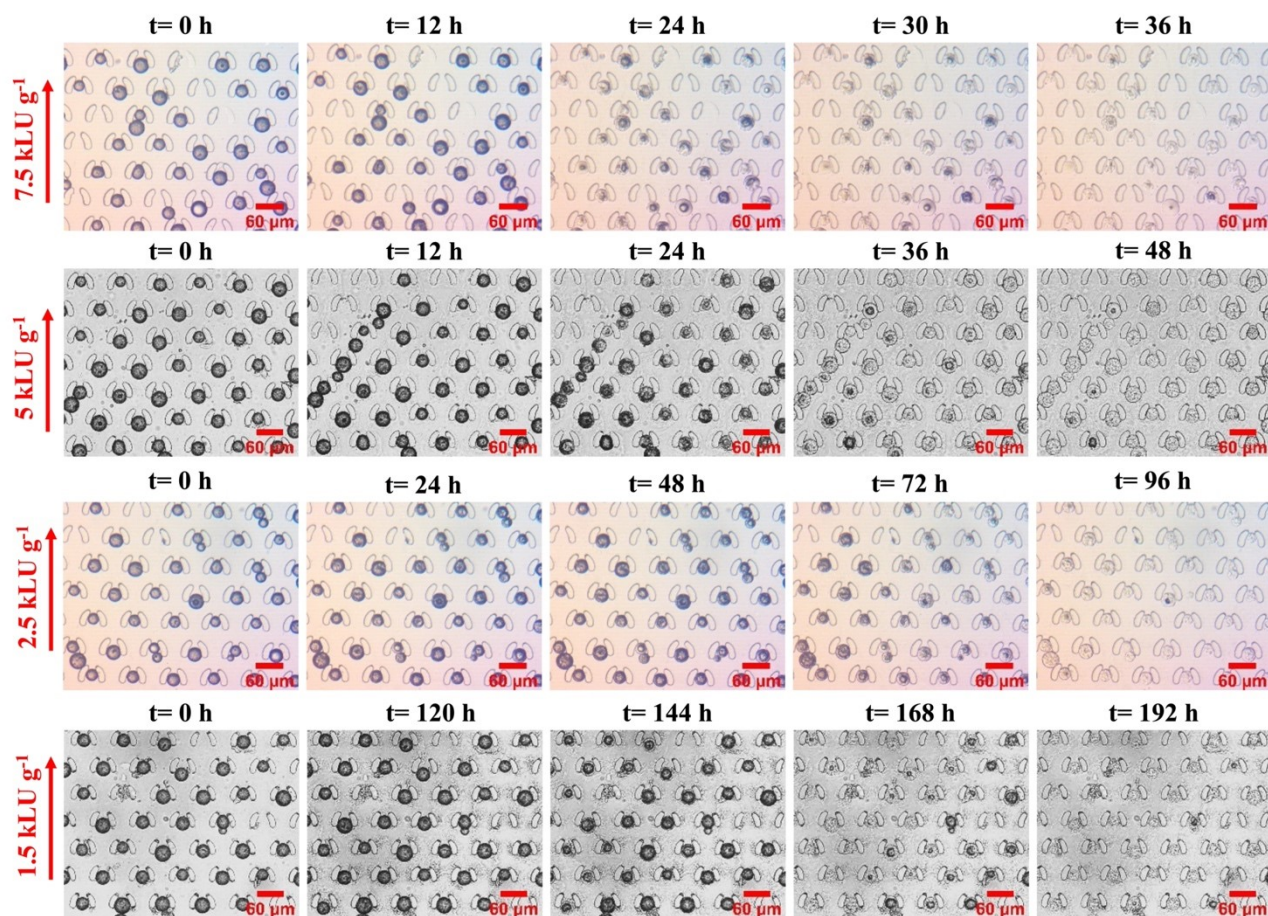**Figure S10:** Time lapse of enzymatic degradation of PBAT microparticles with ~15 μm in radius using enzyme at different concentrations. Scale bar is 60 μm.

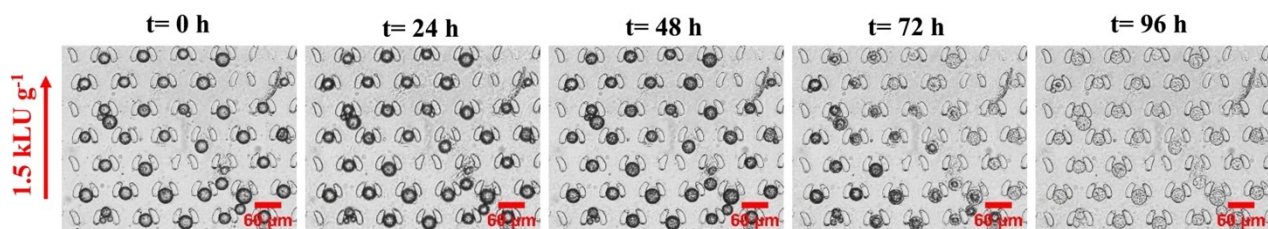**Figure S11:** Time lapse of enzymatic degradation of PBSeT microparticles with ~15 μm in radius using enzyme at 1.5 k LU g-1. Scale bar is 60 μm.
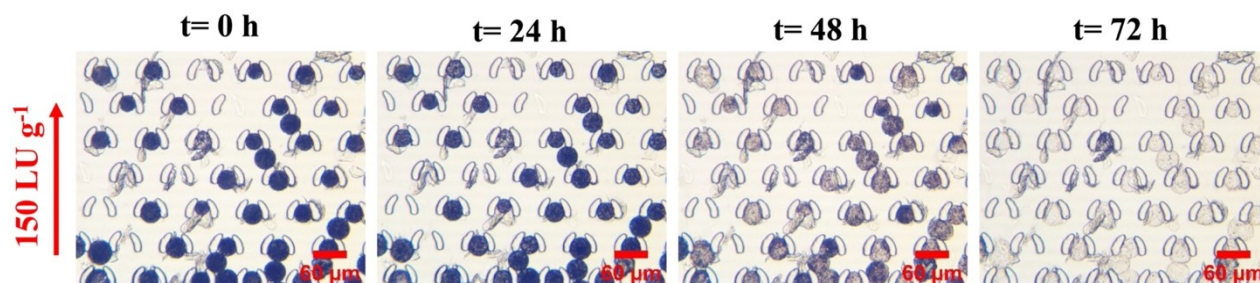
Figure S12: Time lapse of enzymatic degradation of PBS microparticles with ~15 µm in radius using enzyme at 15 LU g-1. Scale bar is 60 µm.
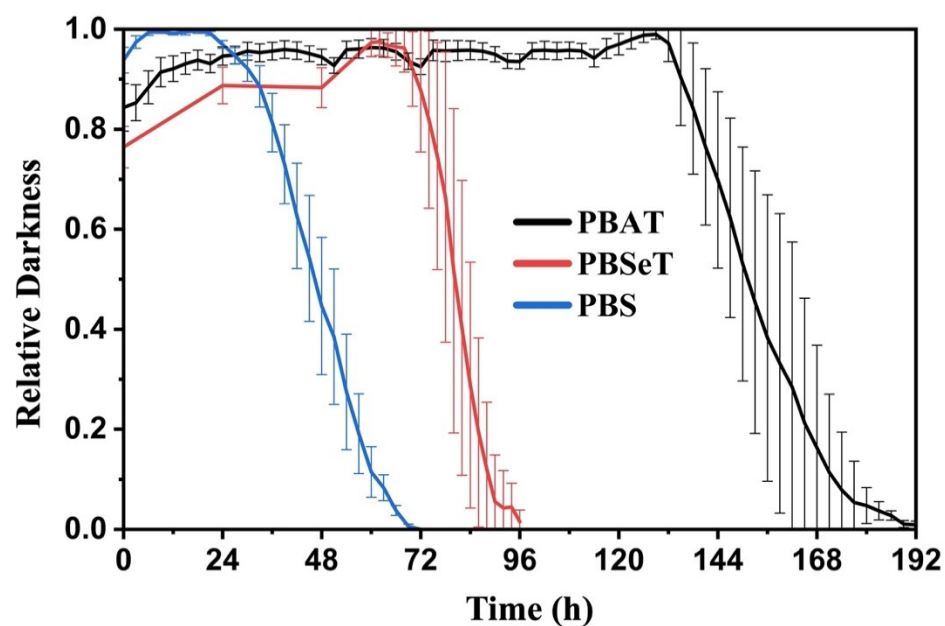

Figure S13: Change in the particles' darkness over time during degradation using enzyme at 1.5 k LU g-1 (PBAT and PBSeT) and 150 LU g^{-1} (PBS)

References

1 F. Barbato, M. I. La Rotonda, G. Maglio, R. Palumbo and F. Quaglia, *Biomaterials*, 2001, **22**, 1371–1378.

2 S. J. Kim, H. W. Kwak, S. Kwon, H. Jang and S. Park, *Polymers*, 2020, **12**, 2389.

3 H. Wang, D. Wei, A. Zheng and H. Xiao, *Polymer Degradation and Stability*, 2015, **116**, 14–22.

4 G. Z. Papageorgiou and D. N. Bikiaris, *Polymer*, 2005, **46**, 12081–12092.

5 C. X. Lam, M. M. Savalani, S.-H. Teoh and D. W. Hutmacher, *Biomedical materials*, 2008, **3**, 034108.

6 G. M. Whitesides, *Annu. Rev. Mater. Sci.*, 1998, **28**, 153.

7 D. Qin, Y. Xia and G. M. Whitesides, *Nature protocols*, 2010, **5**, 491.